

Formation of Ni₃C Nanocrystals by Thermolysis of Nickel Acetylacetonate in Oleylamine: Characterization Using Hard X-ray Photoelectron Spectroscopy

Yuji Goto,[†] Kota Taniguchi,[†] Takahisa Omata,^{*,†} Shinya Otsuka-Yao-Matsuo,[†]
Naoki Ohashi,[‡] Shigenori Ueda,[§] Hideki Yoshikawa,[§] Yoshiyuki Yamashita,[§]
Hirofumi Oohashi,[§] and Keisuke Kobayashi[§]

Division of Materials Science and Manufacturing, Graduate School of Engineering, Osaka University, 2-1 Yamada-oka, Suita, Osaka, 565-0871, Japan, International Center for Nanoarchitectonics (MANA), National Institute for Materials Science (NIMS), 1-1 Namiki, Tsukuba, Ibaraki, 305-0044, Japan, and Department of Materials Infrastructure, National Institute for Materials Science (NIMS), Spring-8, 1-1-1 Kouto, Sayo-cho, Sayo-gun, Hyogo, 679-5148, Japan

Received December 20, 2007. Revised Manuscript Received April 9, 2008

Nickel acetylacetonate was thermally decomposed in oleylamine under inert atmosphere. Nanocrystals of two cubic phases and a hexagonal phase appeared. The phases were identified using X-ray diffraction, laboratory X-ray photoelectron spectroscopy (XPS), and hard-X-ray photoelectron spectroscopy (HX-PES). The hexagonal phase was a nickel carbide, Ni₃C, which had been often identified as a hexagonal close-packed metallic nickel. One cubic phase was a face-centered metallic nickel, and the other cubic phase was proposed as a novel cubic nickel carbide, which was characterized as an intermediate product of the carbidization of metallic face-centered cubic Ni to the hexagonal nickel carbide.

Introduction

Metallic nickel (Ni) has been widely applied to catalysis, electrodes, batteries, permanent magnets, and magnetic recording media. Nanocrystals (NCs) and nanostructured Ni have recently attracted much attention, because of their advanced magnetic and catalytic properties. Ni NCs are usually synthesized by thermal reduction of Ni(II) salts with reducing agents in an organic solvent, e.g., reduction of nickel chloride (NiCl₂) with KBH₄,¹ nickel acetate [Ni(CH₃COO)₂] with tetraethyleneglycol,² nickel carboxylate in an organic amine,³ and so on. In those cases, it is usually observed that thermodynamically stable face-centered cubic nickel (fcc-Ni) is formed at a comparatively low reaction temperature below 240 °C and that metastable hexagonal close-packed nickel (hcp-Ni) appeared at high reaction temperatures above 250 °C. The situation, i.e., the formation temperature of the metastable phase is higher than that of the stable phase, seemed to be a strange phenomenon. Additionally, the magnetic property of the hcp-Ni NCs varied widely in the literature;^{1–3} for example, the saturation magnetization ranged from 0.8 to 30 emu g⁻¹. Meanwhile, there is a report in which the hexagonal phase was not

identified as metallic hcp-Ni but as hexagonal nickel carbide (Ni₃C);⁴ the hexagonal nickel carbide is characterized as an interstitial solid solution of carbon in the metallic hcp-Ni.⁵ This conclusion was derived from the results of laboratory X-ray photoelectron spectroscopy (XPS) using a soft-X-ray as an excitation light source. The information obtained from the XPS does not reflect the bulk states but the near surface states of the materials due to the small escape depth (1–2 nm) of the photoelectrons.⁶ Therefore, it remains an open question whether the hexagonal phase obtained via the solution route is metallic hcp-Ni or nickel carbide. The question should be clarified promptly in order to develop advanced materials consisting of Ni NCs.

Here, we demonstrated the thermolysis of nickel acetylacetonate [Ni(II)(acac)₂] in oleylamine; the synthesis temperature and time varied with the synthesis parameters. The product NCs were characterized by X-ray diffraction (XRD), XPS, hard X-ray photoemission spectroscopy (HX-PES; *hν* = 5946.8 eV), and transmission electron-microscopy (TEM). The HX-PES reflects the bulk states of materials because the photoelectron escape depth is 7–10 nm for ~6 keV photoelectrons, while the XPS using a soft X-ray, such as Al Kα, as an excitation light source is surface-sensitive. The HX-PES results showed that the hexagonal phase was not a metallic hcp-Ni but a hexagonal nickel carbide. The formation mechanism of the hexagonal nickel carbide was proposed, and an unidentified cubic phase was inferred to

* To whom correspondence should be addressed. Tel: +81-6-6879-7462. Fax +81-6-6879-7464. E-mail: omata@mat.eng.osaka-u.ac.jp.

[†] Osaka University.

[‡] International Center for Nanoarchitectonics (MANA), National Institute for Materials Science.

[§] Department of Materials Infrastructure, National Institute for Materials Science.

(1) Mi, Y.; Yuan, D.; Liu, Y.; Zhang, J.; Xiao, Y. *Mater. Chem. Phys.* **2005**, *89*, 359.

(2) Chinnasamy, C. N.; Jeyadevan, B.; Shinoda, K.; Tohji, K.; Narayanasamy, A.; Sato, K.; Hisano, S. *J. Appl. Phys.* **2005**, *97*, 10J309.

(3) Han, M.; Liu, Q.; He, J.; Song, Y.; Xu, Z.; Zhu, J. *Adv. Mater.* **2007**, *19*, 1096.

(4) Leng, Y.; Shao, H.; Wang, Y.; Suzuki, M.; Li, X. *J. Nanosci. Nanotechnol.* **2006**, *6*, 221.

(5) Nagakura, S. *J. Phys. Soc. Jpn.* **1958**, *13*, 1005.

(6) Seah, M. P.; Dench, W. A. *Surf. Interface Anal.* **1979**, *1*, 2.

be cubic nickel carbide, which is an intermediate product of the carbidization of metallic fcc-Ni to the hexagonal nickel carbide.

Experimental Section

Chemicals. Nickel(II) acetylacetonate hydrate [Ni(acac)₂·nH₂O] (Tokyo Chemical Industries, >98%), oleylamine [CH₃(CH₂)₆CH=CH(CH₂)₇NH₂] (Aldrich, 70%), ethanol [C₂H₅OH] (Sigma-Aldrich Japan, >99.5%), and 1-butanol [CH₃(CH₂)₃OH] (Sigma-Aldrich Japan, >99%) were commercially available. The oleylamine was purified by distillation before use. All other chemicals were used without further purification.

Synthesis. The thermolysis of Ni(acac)₂ in oleylamine was performed by the following procedure. A 20.5 mg portion of Ni(acac)₂·nH₂O and 4.0 mL of oleylamine were fed into a glass vial (12 mL capacity). The Ni(acac)₂·nH₂O was dissolved in the oleylamine at 60 °C for 30 min; when the dissolution was completed, the solution became transparent and light-blue-colored. The glass vial was put into a preheated oil-bath; the solution in the vial was heated at 200–320 °C for 30–180 min and then cooled to room temperature. The product precipitates were extracted from the solution by centrifugal separation and successive decantation. The precipitate obtained was washed in a mixed solvent of 1-butanol and ethanol. Successively, the precipitate was washed in hexane and then in chloroform. The washed powder was extracted from the solvent by centrifugal separation and successive decantation. The respective washing processes were repeated several times. Finally, the product powder was dried under vacuum at room temperature.

Characterization. The crystalline phases were identified using powder X-ray diffraction (XRD) (Rigaku, RINT2500, Cu K α radiation using a curved graphite receiving monochromator). Transmission electron microscopic (TEM) observations were carried out using a JEM-2010 (JEOL) operated at 200 kV. Ni 2p and C 1s XPS spectra were recorded using a Rigaku XPS7000 spectrometer with a hemispherical electron analyzer. Al K α radiation ($h\nu = 1486.6$ eV) was used as an excitation source. The NCs were distributed onto a platinum plate and subjected to the XPS measurements. The binding energy was calibrated based on the assumption that the C 1s binding energy for the contaminant carbon is 284.8 eV. High-resolution HX-PES on the Ni 2p and C 1s regions was recorded by a photoelectron spectrometer (VG SCIENTA, SES 2002–6 keV) at the NIMS contract beamline BL15XU of SPring-8; synchrotron radiation ($h\nu = 5946.8$ eV) was used as an excitation light. The powdered sample was distributed onto a conductive carbon tape. The binding energy was calibrated by the Au 4f core level. The XPS and HX-PES measurements were carried out at room temperature. The magnetization curves of the NCs at room temperature were recorded using a vibrating-sample magnetometer (Riken Denshi Co., Ltd., BHV-55). The decomposition behavior upon heating of Ni(acac)₂·nH₂O was studied by thermogravimetry (TG) (Seiko Instruments, TG/DTA320) under Ar gas flow and TG–mass spectroscopy (Rigaku Thermo Mass) under He gas flow.

Results and Discussion

NCs were synthesized by thermolysis of the nickel acetylacetonate in oleylamine in a temperature range between 200 and 320 °C. No product precipitate was obtained for the synthesis at 200 °C; black precipitates were obtained above 240 °C. Figure 1 shows TEM images and the particle size distribution obtained from the TEM observations of the product powders synthesized at 240 and 320 °C for 30 min.

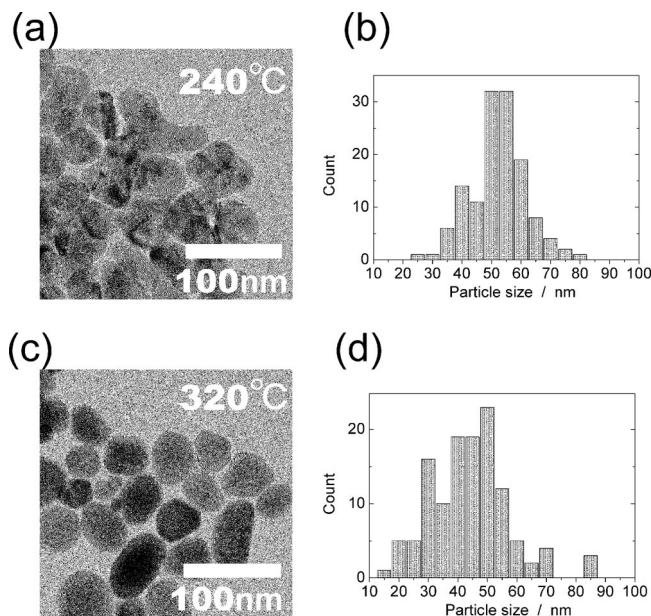


Figure 1. TEM images and particle size distribution evaluated from TEM observations of product NCs: (a and b) 240 °C for 30 min. and (c and d) 320 °C for 30 min.

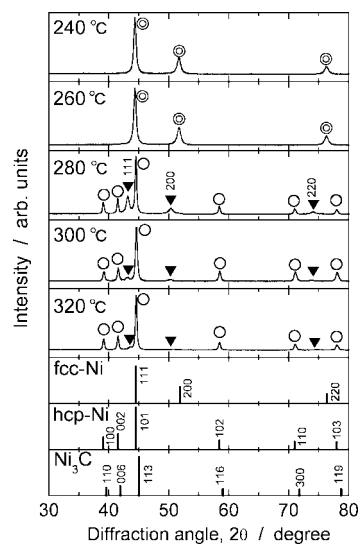


Figure 2. Powder XRD patterns of product NCs together with those of fcc- and hcp-Ni and Ni₃C reported: ⊙, fcc-Ni; ○, hexagonal Ni₃C; and ▼, unidentified cubic phase, which is proposed to be a intermediate cubic nickel carbide. All reaction times were 30 min.

Both the product powders consisted of approximately 50 nm NCs. No distinct crystal growth was observed upon increasing the synthesis temperature. Figure 2 shows X-ray diffraction (XRD) profiles of the product NCs together with the diffraction profiles of metallic fcc-⁷ and hcp-Ni⁸ and hexagonal nickel carbide (Ni₃C).⁵ For the samples synthesized at 240 and 260 °C, the diffractions were indexed as those for the metallic fcc-Ni with a lattice parameter of $a_0 = 353$ pm. For the samples synthesized above 280 °C, diffractions due to fcc-Ni were not observed; a hexagonal phase and a cubic phase appeared. The hexagonal phase (marked by open circles in the figure) was attributed to a

(7) Jette, E. R.; Foote, F. *J. Chem. Phys.* **1935**, *3*, 605.

(8) Weik, H.; Hemenger, P. *Bull. Am. Phys. Soc.* **1965**, *10*, 1140.

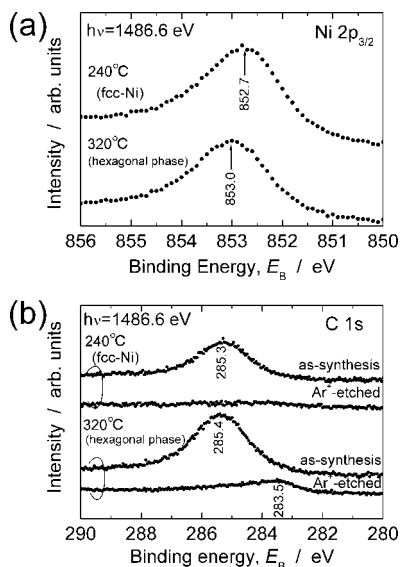


Figure 3. XPS spectra of the product NCs synthesized at 240 and 320 °C for 30 min using Al K α radiation ($h\nu = 1486.6$ eV) as an excitation source: (a) Ni 2p $_{3/2}$ and (b) C 1s regions.

phase possessing the hcp-lattice with lattice parameters of $a_0 = 265$ pm and $c_0 = 434$ pm or the Ni $_3$ C-lattice with $a_0 = 459$ pm and $c_0 = 1303$ pm. The cubic phase (marked by closed triangles in the figure) could be indexed assuming a fcc-lattice with a lattice parameter of $a_0 = 361$ pm. The amount of the cubic phase decreased with increasing synthesis temperature; approximately a single hexagonal phase was obtained at the synthesis temperature of 320 °C. From the XRD results, the hexagonal phase could not be identified as the metallic hcp-Ni or the nickel carbide.

Figure 3 shows the Ni 2p and C 1s core level XPS spectra of the product NCs synthesized at 240 and 320 °C for 30 min. For the Ni 2p region (Figure 3a), the Ni 2p $_{3/2}$ peak was observed at 852.7 eV for the NCs synthesized at 240 °C; the binding energy agreed well with that of the metallic fcc-Ni.⁹ However, for the NCs synthesized at 320 °C, which were identified as hexagonal phase from the XRD results, the binding energy of the Ni 2p $_{3/2}$ was slightly larger than that of the metallic fcc-Ni. For the C 1s region (Figure 3b), a peak at 285.4 eV, which was attributable to the surface contaminant carbon, was observed for both the NCs. After Ar $^+$ -ion etching for 20 s at 400 V acceleration and 400 μ A current, the C 1s peak completely vanished for the metallic fcc-Ni. On the other hand, for the hexagonal phase, a peak positioned at 283.5 eV persisted; the binding energy of 283.5 eV agreed well with that for the Ni–C bond reported.^{10,11} These results were consistent with the literature results reported by Leng et al.⁴

Figure 4 shows the Ni 2p and C 1s core level HX-PES spectra of NCs synthesized under the same conditions as the samples shown in Figure 3. For the NCs synthesized at 240 °C, the Ni 2p $_{3/2}$ peak was observed at 852.7 eV; its binding energy completely agreed with that of metallic fcc-Ni. We

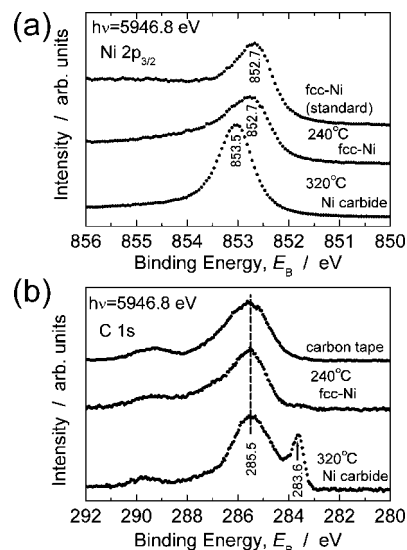


Figure 4. HX-PES spectra of the product NCs synthesized at 240 and 320 °C for 30 min. taken at $h\nu = 5946.8$ eV: (a) Ni 2p $_{3/2}$ and (b) C 1s regions. The NCs were dusted on a carbon adhesive tape in the measurements. The C 1s spectrum of the carbon adhesive tape without NCs is also shown in the figure.

note that no additional C 1s signal in addition to that from the base carbon tape was detected. Therefore, the NCs synthesized at 240 °C were definitely identified as a metallic fcc-Ni. For the NCs synthesized at 320 °C, the Ni 2p $_{3/2}$ peak was observed at 853.5 eV; the binding energy was distinctly higher than that of the metallic fcc-Ni. In contrast to the case of the NCs synthesized at 240 °C, a clear C 1s peak at 283.6 eV was observed, where the C 1s spectrum included the signal from the carbon tape. The binding energy of 283.6 eV agreed with that of the C 1s for the Ni–C bond reported in refs 10, 11. Thus, we concluded that the hexagonal phase for the NCs synthesized at 320 °C was the nickel carbide.

Parts a and b of Figure 5 show magnetization curves of the NCs synthesized at 240 and 320 °C for 30 min, i.e., the metallic fcc-Ni and the hexagonal nickel carbide, respectively. For the fcc-Ni NCs, the hysteresis loop indicated ferromagnetic behavior with a saturation magnetization of 41.5 emu g $^{-1}$; the saturation magnetization was consistent with that previously reported in ref 4. For the hexagonal nickel carbide NCs, the saturation magnetization (0.26 emu g $^{-1}$) was approximately the same as the value of ~ 0.8 emu g $^{-1}$,³ which was the value for the alleged metallic hcp-Ni NCs. Another saturation magnetization value of ~ 7 emu g $^{-1}$ was reported for the hcp-Ni NCs synthesized via the organic solution route;¹ the value was significantly larger than and inconsistent with the present saturation magnetization for the nickel carbide NCs. It has been predicted on the basis of the electronic band calculation that the hexagonal Ni $_3$ C is not ferromagnetic.¹² Although the magnetic properties of the nickel carbide should be dependent on the carbon concentration and the particle size, we inferred that the ferromagnetic behavior observed in Figure 5b was due to the contaminant metallic fcc-Ni. When the metallic fcc-Ni is present in the nickel carbide as a contaminant, the M – H curve should vary

(9) Moulder, J. F.; Stickle, W. F.; Sobol, P. E.; Bomben, K. D. *Handbook of X-ray Photoelectron Spectroscopy*; Physical Electronics, Inc.: Chanhassen, MN, 1995.

(10) Ujvari, T.; Toth, A.; Kovacs, Gy. J.; Safran, G.; Geszti, O.; Radnoczi, G.; Bertoti, I. *Surf. Interface Anal.* **2004**, *36*, 760.

(11) Wiltner, A.; Linsmeier, Ch. *Phys. Status Solidi A* **2004**, *201*, 881.

(12) Yue, L.; Sabirianov, R.; Kirkpatrick, E. M.; Leslie-Pelecky, D. L. *Phys. Rev. B* **2000**, *62*, 8969.

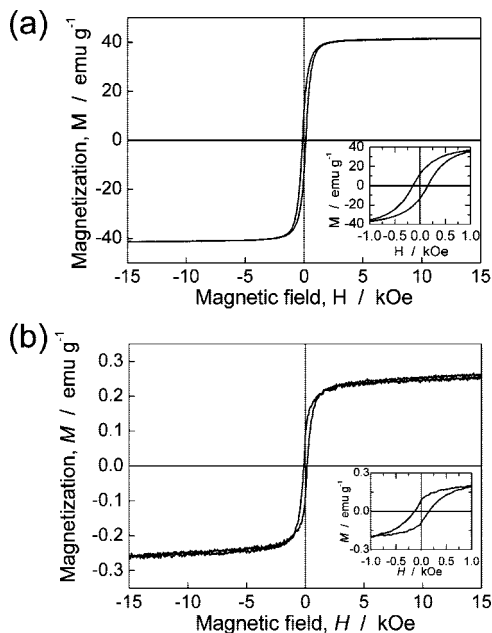


Figure 5. Hysteresis curve ($M-H$) of the product NCs: (a) synthesized at 240 °C for 30 min. (fcc-Ni NCs) and (b) synthesized at 320 °C for 30 min. (hexagonal Ni carbide NCs).

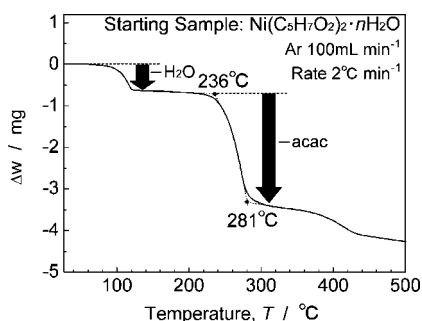


Figure 6. The result of thermal gravimetric (TG) analysis of Ni acetylacetonate in flowing Ar gas.

depending on the concentration of the contaminant fcc-Ni. The variation of the saturation magnetization previously reported for the alleged hcp-Ni can be explained as the samples measured being hexagonal nickel carbide, Ni_3C , NCs with various concentrations of contaminant fcc-Ni.

Figure 6 shows the result of TG analysis of $\text{Ni}(\text{acac})_2 \cdot n\text{H}_2\text{O}$ heated under Ar atmosphere. The $\text{Ni}(\text{acac})_2 \cdot n\text{H}_2\text{O}$ released its hydrated water at ~ 100 °C. The acetylacetonate was decomposed and released above 236 °C, and the mass steeply decreased up to 281 °C. The decomposition and release of acetylacetonate were almost completed at ~ 280 °C. During the $\text{Ni}(\text{acac})_2$ decomposition, significant CO gas evolution was detected by TG–mass spectroscopy analysis; CO gas evolution during the thermal decomposition of carboxylates is common understanding.¹³ Therefore, the carbidization of metallic Ni occurs by exposure to CO gas.⁵ Taking into account the CO gas evolution during decomposition of the acetylacetonate, the TG curve explained well the present phase transformation of NCs as follows: Since the decomposition of acetylacetonate did not start below 220

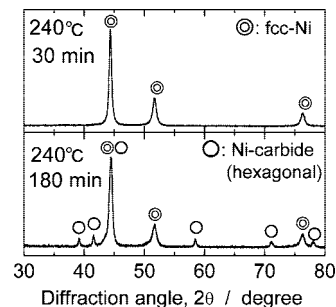


Figure 7. XRD profiles of the product NCs synthesized at 240 °C for 30 and 180 min. The NCs synthesized at 240 °C for 180 min were identified as a mixed phase of metallic fcc-Ni and hexagonal nickel carbide: ⊙, fcc-Ni; ○, hexagonal Ni_3C .

°C, no precipitated product was obtained at 200 °C, and precipitates appeared above 240 °C. The decomposition of acetylacetonate occurred moderately and the CO gas was evolved very slowly below 260 °C; therefore, the metallic nickel NCs were formed because of avoidance of carbidization. Since the crucial CO gas evolution occurred above 280 °C due to the strongly accelerated decomposition of acetylacetonate, the carbidization of metallic nickel occurred by exposure to the CO gas. As a result, the product NCs became nickel carbide. In this interpretation of the nickel carbide formation, we assumed that metallic nickel formed at first and then its carbidization occurred. The validity of the assumption was demonstrated by the change of the product phase depending on the reaction time, as shown in Figure 7. Only the metallic fcc-Ni was obtained for the synthesis at 240 °C for 30 min; the hexagonal nickel carbide appeared with increasing the reaction time up to 180 min. On the basis of this carbidization mechanism, it is plausible that the cubic nickel carbide (Ni–C alloy), which should be characterized as an interstitial solid solution of carbon in fcc-Ni, appears as an intermediate product from the fcc-Ni to the hexagonal nickel carbide. It was reported by Zwell et al. that the dissolution of carbon into fcc-Ni occurs and that the dissolution of carbon into fcc-Ni expands the fcc lattice.¹⁴ For instance, the lattice parameter increased from 352.37 pm for the fcc-Ni to 353.49 pm for the cubic Ni–C alloy containing 1.47 atom % carbon. On the basis of the situation, the unidentified cubic phase appearing above 280 °C (marked by closed triangles in Figure 2) was attributable to the heavily carbon dissolved fcc-Ni, i.e., a cubic nickel carbide, because of its larger lattice parameter ($a_0 = 361$ pm) than that of metallic fcc-Ni ($a_0 = 353$ pm). However, further study, such as the isolation of the cubic phase and its structural refinement, is required in order to obtain the evidence that the cubic phase observed in Figure 2 is identified as an intermediate cubic nickel carbide.

Conclusion

In summary, the NCs phases obtained from the thermolysis of nickel acetylacetonate in oleylamine have been identified using XPS, HX-PES, and XRD. The alleged metastable metallic hcp-Ni turned out to be a hexagonal nickel carbide,

(13) Mohamed, M. A.; Halawy, S. A.; Ebrahim, M. M. *J. Anal. Appl. Pyrol.* **1993**, *27*, 109.

(14) Zwell, L.; Fasiska, E. J.; Nakada, Y.; Keh, A. S. *Trans. Metall. Soc. AIME* **1968**, *242*, 765.

Ni₃C. The formation mechanism of the hexagonal nickel carbide proposed is summarized as follows: The metallic fcc-Ni NCs are formed by the thermal decomposition of the acetylacetonate and reduction of Ni(II) at first, and then carbidization into hexagonal nickel carbide occurs; the cubic nickel carbide is probably formed as an intermediate product. The carbidization of the fcc-Ni progresses by exposure to the CO gas that is emitted during the acetylacetonate decomposition above ~240 °C. The previously reported solution syntheses of the alleged metallic hcp-Ni were carried out using solutions containing some organic reagents such as amines, glycols, and so on, where the reaction temperature was usually above 250 °C. Under such reaction conditions, some organic reagents should decompose and CO gas forms, and the product metallic fcc-Ni NCs exposed to the CO gas should undergo carbidization. Thus, we conclude that the alleged metastable hcp-Ni in the previous work involves certain carbon contamination, and it becomes practically the nickel carbide.

Acknowledgment. The authors would like to express our grateful acknowledgement to Mr. Daisuke Nomoto, Dr. Yoshio Katsuya, and the staff of the SPring-8, for their help with the HX-PES experiments; Dr. Masato Ueda, for his help with the TEM observation; and Prof. Ryoichi Nakatani and Dr. Yu Shiratsuchi, for their help with the VSM measurements. The authors are grateful to Dr. M. Arita, Prof. K. Shimada, and Prof. H. Namatame of HiSOR, Hiroshima University, and Dr. Y. Takeda and Dr. Y. Saitoh of JAEA/SPring-8 for their contribution to the construction of the HX-PES experimental station at BL15XU of SPring-8. The HX-PES measurements were performed under the approval of NIMS Beamline Station (Proposal No. 2007A4609). H.O. has been supported by the Nanotechnology-Network Project of the Ministry of Education, Culture, Sports, Science and Technology in Japan. The authors thank Rigaku Corp. for the TG–mass spectroscopy measurement. This work was supported in part by a Grant-in-Aid for Scientific Research on Priority Area, “Nanoionics (439)” (Grant No. 17041010 and 19017013) by the Ministry of Education, Culture, Sports and Technology, Japan.

CM703644X